

Differential X-ray Absorption and Dust-To-Gas Ratios of the Lens Galaxies SBS 0909+523, FBQS 0951+2635, and B 1152+199

Xinyu Dai¹ and Christopher S. Kochanek¹

ABSTRACT

We analyzed *Chandra* observations of three gravitational lenses, SBS 0909+523, FBQS 0951+2635, and B 1152+199, to measure the differential X-ray absorption and the dust-to-gas ratio of the lens galaxies. We successfully detected the differential X-ray absorption in SBS 0909+523 and B 1152+199, and failed to detect it in FBQS 0951+2635 due to the dramatic drop in its flux from the *ROSAT* epoch. These measurements significantly increase the sample of dust-to-gas ratio measurements in cosmologically-distant, normal galaxies. Using the larger sample, we obtain an average dust-to-gas ratio of $E(B - V)/N_{\text{H}} = (1.5 \pm 0.5) \times 10^{-22} \text{ mag cm}^2 \text{ atoms}^{-1}$ with an estimated intrinsic dispersion in the ratio of $\simeq 40\%$. This average dust-to-gas ratio is consistent with our previous measurement, and the average Galactic value of $1.7 \times 10^{-22} \text{ mag cm}^2 \text{ atoms}^{-1}$ and the estimated intrinsic dispersion is also consistent with the 30% observed in the Galaxy. A larger sample size is still needed to improve the measurements and to begin studying the evolution in the ratio with cosmic time. We also detected X-ray microlensing in SBS 0909+523 and significant X-ray variability in FBQS 0951+2635.

Subject headings: galaxy: evolution – ISM: dust-to-gas ratio

1. Introduction

The inter-stellar medium (ISM) and inter-galactic medium (IGM) are ubiquitous, and understanding the ISM is crucial to many areas of astronomy such as cosmology (e.g., using SNe Ia or GRBs as cosmological probes), the evolution of galaxies, and star formation (e.g., Fall et al. 1996; Madau et al. 1998; Schneider et al. 2004; Corasaniti 2006; Ghirlanda et al. 2006; Lacey et al. 2008). The dust-to-gas ratio is a basic property of the

¹Department of Astronomy, The Ohio State University, Columbus, OH 43210, xinyu@astronomy.ohio-state.edu, ckochanek@astronomy.ohio-state.edu

ISM, and it is difficult to measure in distant galaxies. In the Galaxy, it is measured by comparing the optical extinction and Ly α absorption towards stars, and a typical value is $E(B - V)/N_{\text{H}} = 1.7 \times 10^{-22} \text{ mag cm}^2 \text{ atoms}^{-1}$ with a scatter about the mean of order 30% (Bohlin, Savage & Drake 1978). Subsequent studies have extended these measurements to additional lines of sight in our Galaxy and to the LMC and SMC, but the basic results are little altered aside from some evidence that the dust-to-gas ratios of the LMC and SMC are modestly lower ($\sim 30\%$) than in the Galaxy (see the review by Draine 2003 and references therein). This absorption method is hard to apply to extragalactic sources where we lack precise knowledge of the intrinsic source spectra and tend to be probing low density parts of the IGM using absorption lines in the spectra of quasars or γ -ray bursts (e.g., Kacprzak et al. 2008) rather than the inner regions of normal galaxies. An alternate approach is to use emission by the dust in the far-infrared to estimate a dust mass and then compare it to the estimated gas mass (e.g., Contini & Contini 2007).

Gravitational lensing provides a means of studying the properties of the ISM through differential absorption in the lens galaxies between the locations of the quasar images. By studying the *differences* in the absorption (or extinction) between multiple images, any contamination from the Galaxy in the foreground (Milky Way) or the quasar host galaxy in the background is essentially eliminated and we can be confident that we are probing the ISM of the lens galaxy. Moreover, since we are comparing two images of the same quasar, the method has many of the quantitative advantages of the local approach using stars of known spectral type. In optical bands, this technique has been widely used to study dust extinction and the dust extinction law in lens galaxies (e.g., Nadeau et al. 1991; Falco et al. 1999; Toft, Hjorth & Burud 2000; Motta et al. 2002; Wucknitz et al. 2003; Muñoz et al. 2004; Mediavilla et al. 2005; Elíasdóttir et al. 2006). In X-rays, Dai et al. (2003) and Dai & Kochanek (2005) measured the differential column densities in two lenses Q 2237+0305 and B 1600+434. Subsequently, Dai et al. (2006) expanded the results to four lenses and proposed that the evolution of the dust-to-gas ratio can be determined given a larger sample. In this paper, we present new measurements based on *Chandra* observations of the quasar lenses SBS 0909+523 (Kochanek et al. 1997), FBQS 0951+2635 (Schechter et al. 1998), and B 1152+199 (Myers et al. 1999).

2. Observations and Data Reduction

We observed SBS 0909+523 and FBQS 0951+2635 with the Advanced CCD Imaging Spectrometer (ACIS, Garmire et al. 2003) on board *Chandra* (Weisskopf et al. 2002) for 19.6 and 34.2 ks on December 17, 2006 and March 24, 2007, respectively. B 1152+199 was

observed in a separate program (PI: K. Pedersen) with *Chandra*-ACIS for 16.4 and 8.3 ks on February 22, 2005 and February 26, 2005. The back-side illuminated S3 chip was used in all the observations. A journal of the *Chandra* observations is presented in Table 1. The *Chandra* data were reduced using the CIAO 4.0 software tools provided by the *Chandra* X-ray Center (CXC), following the standard threads on the CXC website.¹ We used the most recently reprocessed data products (Reprocessing III) and calibration files (CALDB 3.4.2). Only events with standard *ASCA* grades of 0, 2, 3, 4, and 6 were used in the analysis. We improved the image quality of the data by removing the pixel randomization applied to the event positions by the standard pipeline. In addition, we applied a subpixel resolution technique (Tsunemi et al. 2001; Mori et al. 2001) to the events on the S3 chip of ACIS where the lensed images are located. Figure 1 shows the resulting images.

3. Spectral Analysis

We fit the spectra of the lensed quasars using XSPEC V11.3.1 (Arnaud 1996) over the 0.3–8 keV observed energy range. The X-ray spectrum of the i th image was modeled as

$$N_i(E, t) = N_{0,i}(t - \Delta t_i) \left(\frac{E}{E_0} \right)^{-\Gamma(t - \Delta t_i)} \exp \left\{ -\sigma(E) N_{H,Gal} - \sigma [E(1 + z_l)] N_{H,i} - \sigma [E(1 + z_s)] N_{H,Src}(t - \Delta t_i) \right\}, \quad (1)$$

where $N_i(E, t)$ is the number of photons per unit energy interval, $N_{H,Gal}$, $N_{H,i}$, and $N_{H,Src}$ are the equivalent hydrogen column densities in our Galaxy, the lens galaxy at the position of image i , and in the source galaxy, respectively, $\sigma(E)$ is the photo-electric absorption cross-section, and Δt_i is the time-delay. Although, absorption by the Galaxy, lens and source is

¹The CXC website is at <http://cxc.harvard.edu/>.

Table 1. *Chandra* Observations of Gravitational Lenses SBS 0909+523, FBQS 0951+2635, and B 1152+199.

Lenses	Date	Exp (sec)	Count Rate (ct/s, 0.3–8 keV)	Raw Flux Ratio (A/B) ^a
SBS 0909+523	2006-12-17	19654	0.162 ± 0.003	0.34 ± 0.02
FBQS 0951+2635	2007-03-24	34243	0.0074 ± 0.0005	5.2 ± 1.4
B 1152+199	2005-02-22	16449	0.189 ± 0.003	3.06 ± 0.14
B 1152+199	2005-02-26	8282	0.198 ± 0.005	3.83 ± 0.26

^aThe raw flux ratio has not been corrected for the differential absorption between the two images.

degenerate when fitting the spectrum of each image, the differential absorption ΔN_{H} between the lensed images is not and can be determined from a simultaneous fit to the spectra of the images. The time-delay at the source complicates the measurement, since if the absorption at source is variable (e.g., PKS 1830–211, Dai et al. 2008), it will not be exactly canceled when comparing the two spectra. However, since the photo-electric absorption cross-section decreases with energy $\sigma(E) \propto E^{-3}$, the absorption at the source will affect the spectrum less. Thus, we neglected the time-delay between the images and the absorption at the source redshift in this analysis. We note that a significant change in the spectral index on the time scale of the time delays will affect the results, especially for quasars with poor S/N spectra where the spectral index is degenerate with the absorption. The problem is less severe for quasars with moderate to high S/N spectra where the spectral index is less degenerate with N_{H} absorption during spectral modeling.

A second systematic error we must consider is microlensing of the quasar by the stars in the lens galaxy. Our analysis is only affected by chromatic microlensing, where there are significant changes in the optical and X-ray spectra that alter the estimated extinction or absorption. Indeed, it needs only be achromatic “locally” to separate optical and X-ray wavelength/energy regimes, as global shifts of the optical spectrum relative to the X-ray spectrum by microlensing also have no effect on the results. For the systems we consider, we have only limited control on the level of microlensing. While X-ray microlensing has been detected (Chartas et al. 2002, 2007; Dai et al. 2003; Blackburne et al. 2006; Pooley et al. 2007), X-ray spectral changes due to microlensing have yet to be detected in large part due to the limited sensitivity of the data. Chromatic microlensing in the optical has been observed (Poindexter et al. 2007; Anguita et al. 2008; Eigenbrod et al. 2008) and can create systematic problems for estimates of the extinction as we had already discovered for HE 1104–1805 (Dai et al. 2006). We can, however, compare the optical and X-ray flux ratios, since the evidence to date is that the X-ray sources are much more compact than the optical (Kochanek et al. 2006; Morgan et al. 2008; Chartas et al. 2008) and so more strongly affected by microlensing. If the extinction and absorption-corrected flux ratios of the images agree, this is a good indication that our estimates are little affected by microlensing.

We used the standard `wabs` and `zwabs` models in `XSPEC` to model the Galactic absorption and absorption at the lens redshift. The `wabs` and `zwabs` models use cross sections from Morrison & McCammon (1983) and assume a solar elemental abundance from Anders & Ebihara (1982). The Galactic N_{H} is fixed using the values from Dickey & Lockman (1990). We fixed the intrinsic power-law index Γ to be the same for both lensed images, and allowed the absorption at the lens to differ. Since the average lens absorption and the power-law index are correlated in the spectral modeling, the uncertainties in absorption by the lens for the individual images are correlated. To accurately measure the uncertainties in the

differential absorption, we used XSPEC to explore the full parameter space of the lens column densities and the power-law index. The fitting results are listed in Table 2, and the spectra and best fit models are shown in Figures 2, 3, and 4. We also obtained the unabsorbed flux ratios between the quasar images as part of the model, and verified that adding absorption in the source does not alter the estimates of the differential column densities. We describe the results for each of the three lenses in the following sub-sections.

3.1. SBS 0909+523

SBS 0909+523 (Kochanek et al. 1997; Oscoz et al. 1997) is a two-image lens system with a source redshift of $z_s = 1.377$ and a lens redshift of $z_l = 0.83$. SBS 0909+523 is well studied in the optical bands, and the extinction curve has been measured using the differential extinction method (Mediavilla et al. 2005) to be a Galactic extinction curve with a strong 2175Å extinction feature (Motta et al. 2002).

It is clear from the *Chandra* spectra that image B is more heavily absorbed than image A. We estimate that the difference in the column densities is $\Delta N_{\text{H}B,A} = (0.055_{-0.022}^{+0.095}) \times 10^{22} \text{ cm}^{-2}$. There are several differential extinction measurements for this system (Falco et al. 1999; Motta et al. 2002; Mediavilla et al. 2005), and we used the most recent measurement, $\Delta E(B - V) = 0.32 \pm 0.01$, from Mediavilla et al. (2005). Combined with our differential absorption measurement, we obtained a dust-to-gas ratio of $E(B - V)/N_{\text{H}} = (5.8_{-3.7}^{+3.9}) \times 10^{-22} \text{ mag cm}^2 \text{ atoms}^{-1}$.

The optical flux ratio of SBS 0909+523 has changed little from its discovery in 1997 through 2006 (Kochanek et al. 1997; Motta et al. 2002; Goicoechea et al. 2008) suggesting that there is little microlensing variability even if there is evidence for microlensing from the difference between the continuum and emission line flux ratios (Motta et al. 2002; Mediavilla et al. 2005). The extinction and absorption corrected optical ($A/B = 0.35 \pm 0.02$, Mediavilla et al. 2005) and X-ray flux ratios ($A/B = 0.32 \pm 0.03$) are consistent but differ from the *H*-band ($A/B = 1.12$, Lehar et al. 2000) and extinction-corrected emission line flux ratios (Mediavilla et al. 2005), indicating that there is microlensing in this system but it is affecting the optical and X-ray similarly. The lack of variability and the similar optical/X-ray flux ratios suggests the lens is in a region of relatively uniform microlensing magnification. We also note that the X-ray variability of the source is modest. SBS 0909+523 was observed three times by *ROSAT*, and the source showed moderate X-ray variability of about 40% (Chartas 2000). The flux observed by *Chandra* is in between the three *ROSAT* flux measurements, suggesting no significant total X-ray variability.

Table 2. Spectral Fitting Results

Quasar	Model ^a	Galactic N_{H} (10^{22} cm $^{-2}$)	N_{H} (B - A) (10^{22} cm $^{-2}$)	Γ	Flux Ratio (A/B)	χ^2 (dof)	C-Stat(dof)
SBS 0909+523	wabs(zwabs(pow))	0.0169 (fixed)	$0.055^{+0.095}_{-0.022}$	1.63 ± 0.05	0.32 ± 0.03	124.5(148)	...
FBQS 0951+2635	wabs(zwabs(pow))	0.0229 (fixed)	$0.49^{+0.49}_{-0.41}$	1.32 (fixed) ^b	3.5 ± 1.6	...	56.9(29)
B 1152+199 (Epoch I)	wabs(zwabs(pow))	0.0273(fixed)	0.48 ± 0.06	2.08 ± 0.05	1.87 ± 0.14	148.23(136)	...
B 1152+199 (Epoch II)	wabs(zwabs(pow))	0.0273(fixed)	0.48 ± 0.08	2.10 ± 0.05	2.28 ± 0.25	54.8(75)	...
B 1152+199 (Combined)	wabs(zwabs(pow))	0.0273(fixed)	0.48 ± 0.04	2.07 ± 0.03	...	213.1(217)	...

Note. — Simultaneous fits to the individual spectra of the lensed quasars. The spectra are constrained to have the same intrinsic power-law photon index but can have different absorption column densities at the redshift of the lens.

^aWabs, zwabs, and pow are the XSPEC models used for the Galactic absorption, absorption at the lens, and the intrinsic power-law spectrum, respectively.

^bThe photon index is fix to the best fit value performed in the 2–8 keV.

3.2. FBQS 0951+2635

FBQS 0951+2635 is a two-image lens discovered by Schechter et al. (1998) with a source redshift of $z_s = 1.24$ and a lens redshift of $z_l = 0.26$ (Eigenbrod et al. 2007). FBQS 0951+2635 was detected in the *ROSAT* All Sky Survey (RASS) with a count rate of 0.02 ct s^{-1} in the 0.1–2.4 keV band (Voges et al. 2000). Our *Chandra* image shows that FBQS 0951+2635 is the brightest source within a $2'$ radius circle, which indicates that the source detected in RASS is FBQS 0951+2635. However, the *Chandra* count rate of FBQS 0951+2635, 0.007 ct s^{-1} in the 0.3–8 keV band, is significantly lower than the predicted count rate (0.06 ct s^{-1}) from the RASS, suggesting significant source variability.

The unexpected drop in flux resulted in low S/N spectra that cause significant challenges in measuring the differential absorption. We used the C-statistic (Cash 1979), suitable for small number statistics, to fit the spectra. Using our standard technique, we found a power-law index of $\Gamma = 0.81 \pm 0.15$ for the source. We failed to detect the differential absorption in this lens, as the differential absorption between the two images is consistent with zero. Note, however, that the upper limit for the lens absorption in image B, $N_{\text{HB}} < 0.22 \times 10^{22} \text{ cm}^{-2}$ is larger than that for image A, $N_{\text{HA}} < 0.05 \times 10^{22} \text{ cm}^{-2}$, and that the best fit power-law index ($\Gamma = 0.81 \pm 0.15$) is unusually flat (e.g., Reeves & Turner 2000; Saez et al. 2008). A more plausible interpretation is that the low energy part of the spectrum is absorbed. Since the absorption is correlated with the power-law index in the spectral fitting, which is a severe problem for low S/N spectra, as an experiment we first fit the spectra in the hard band (2–8 keV) to find a steeper, and more sensible, intrinsic power-law ($\Gamma = 1.32$). Then we held this fixed and fit for the absorption to find a differential absorption of $\Delta N_{\text{HB,A}} = (0.49_{-0.41}^{+0.49}) \times 10^{22} \text{ cm}^{-2}$. Due to the low significance of this detection (or non-detection at all) because of the low S/N spectra, we will be unable to include this lens in an estimate of the mean dust-to-gas ratio.

3.3. B 1152+199

B 1152+199 (Myers et al. 1999) consists of two $z_s = 1.019$ quasar images lensed by a $z_l = 0.439$ galaxy. The dust extinction curve of B 1152+199 was measured to be $1.3 \leq R_V \leq 2.0$ (Toft et al. 2000) and $R_V = 2.1 \pm 0.1$ (Elíasdóttir et al. 2006). The Elíasdóttir et al. (2006) results were based on improved data so we adopt their results. The differential absorption can be clearly seen by comparing the *Chandra* spectra of the two images (Figure 4). Since B 1152+199 was observed by *Chandra* twice, we used our standard method and simultaneously fit the spectra for both epochs. We detected a large differential absorption $\Delta N_{\text{HB,A}} = (0.48 \pm 0.04) \times 10^{22} \text{ cm}^{-2}$. We also fit the two *Chandra* epochs

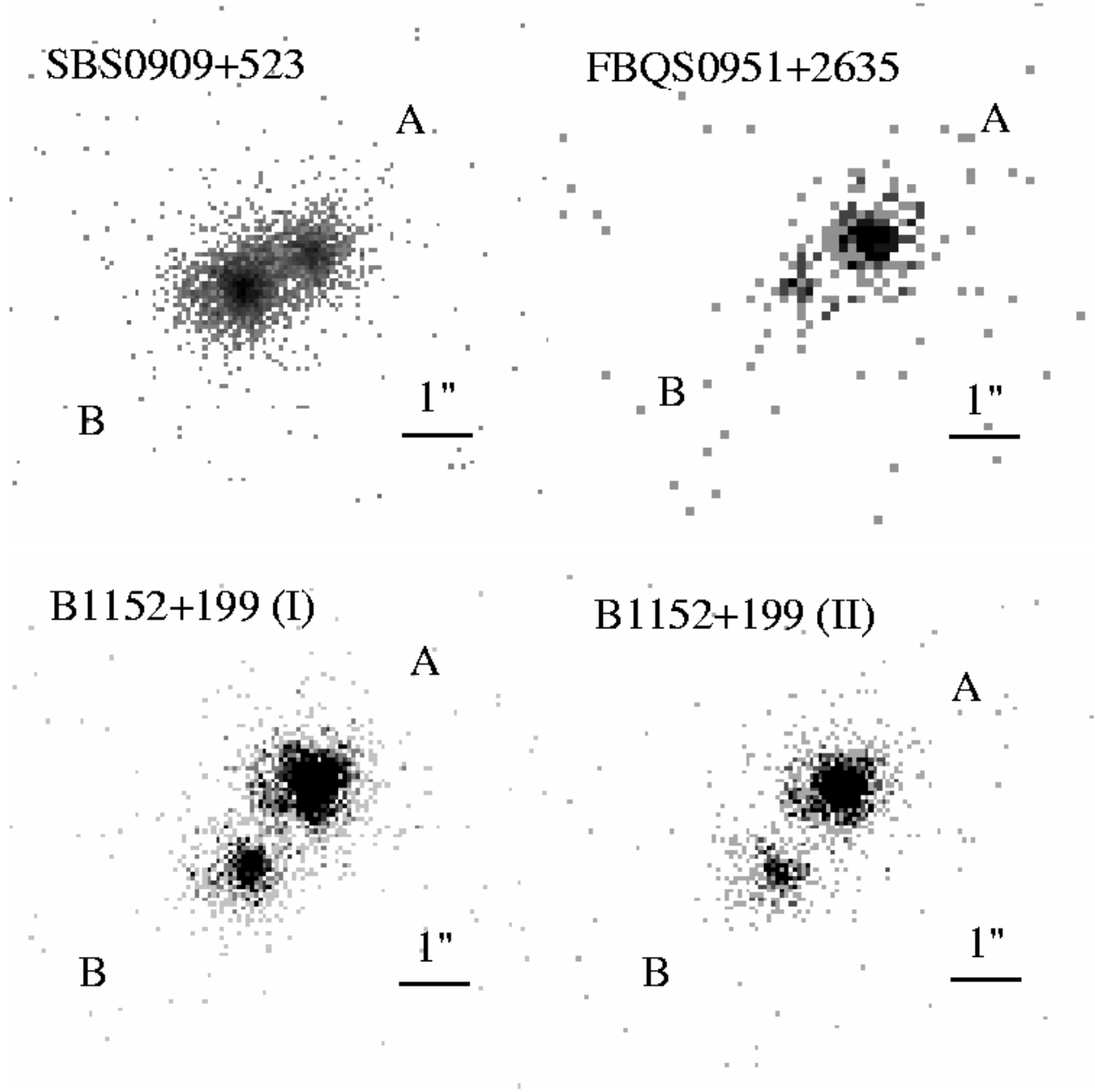


Fig. 1.— *Chandra* images of SBS 0909+523, FBQS 0951+2635, and B 1152+199.

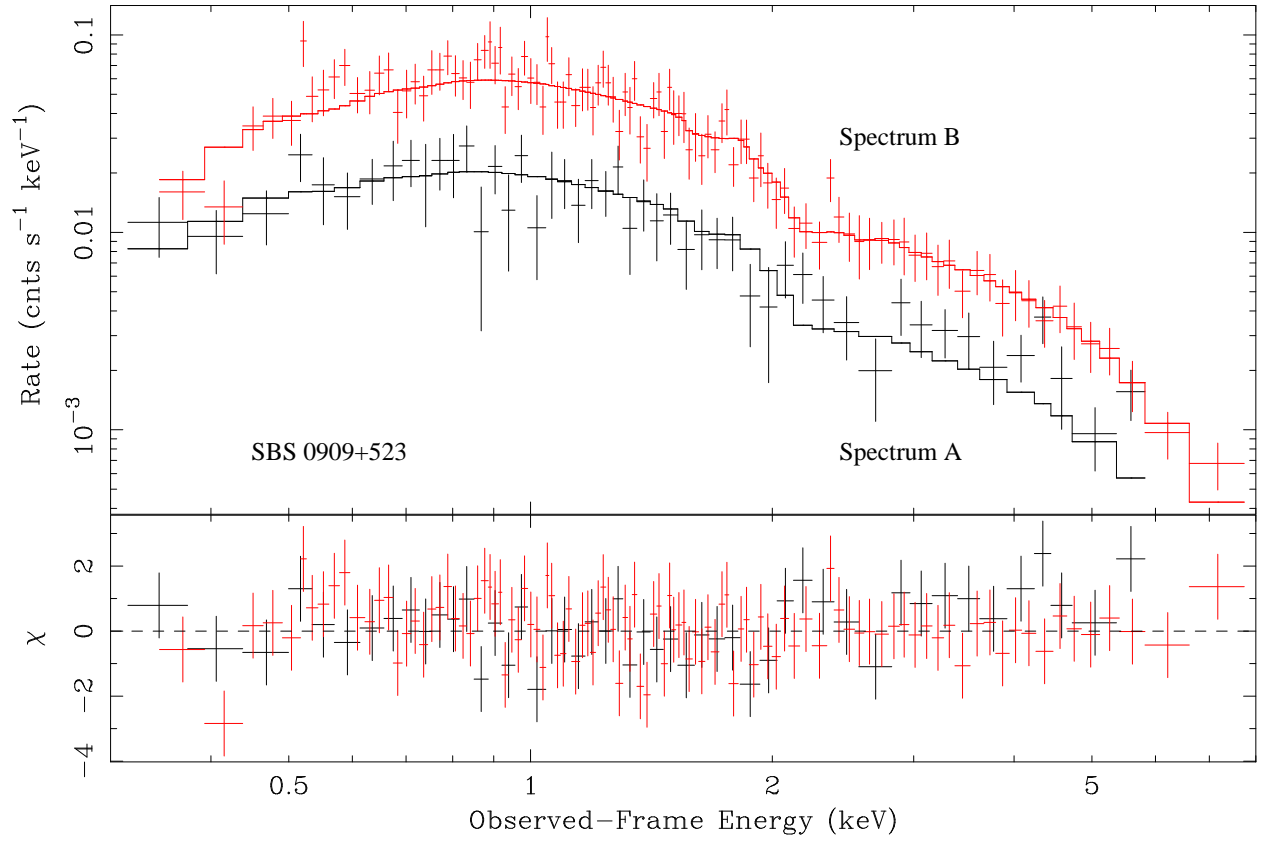


Fig. 2.— Spectra of images A (bottom) and B (top) of SBS 0909+523. The lower panel shows the contributions of the residuals to the χ^2 fit statistics.

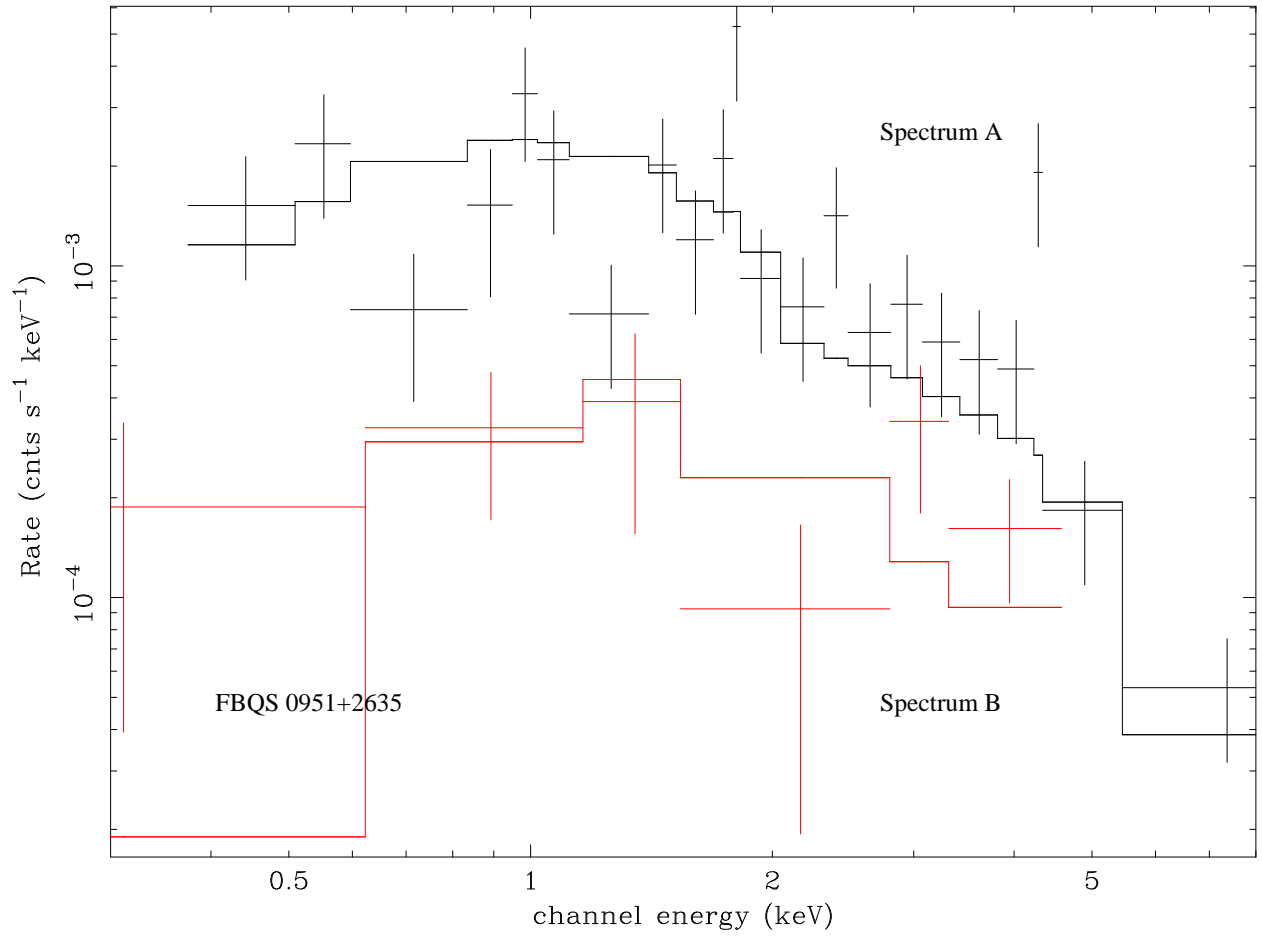


Fig. 3.— Spectra of images A (top) and B (bottom) of FBQS 0951+2635.

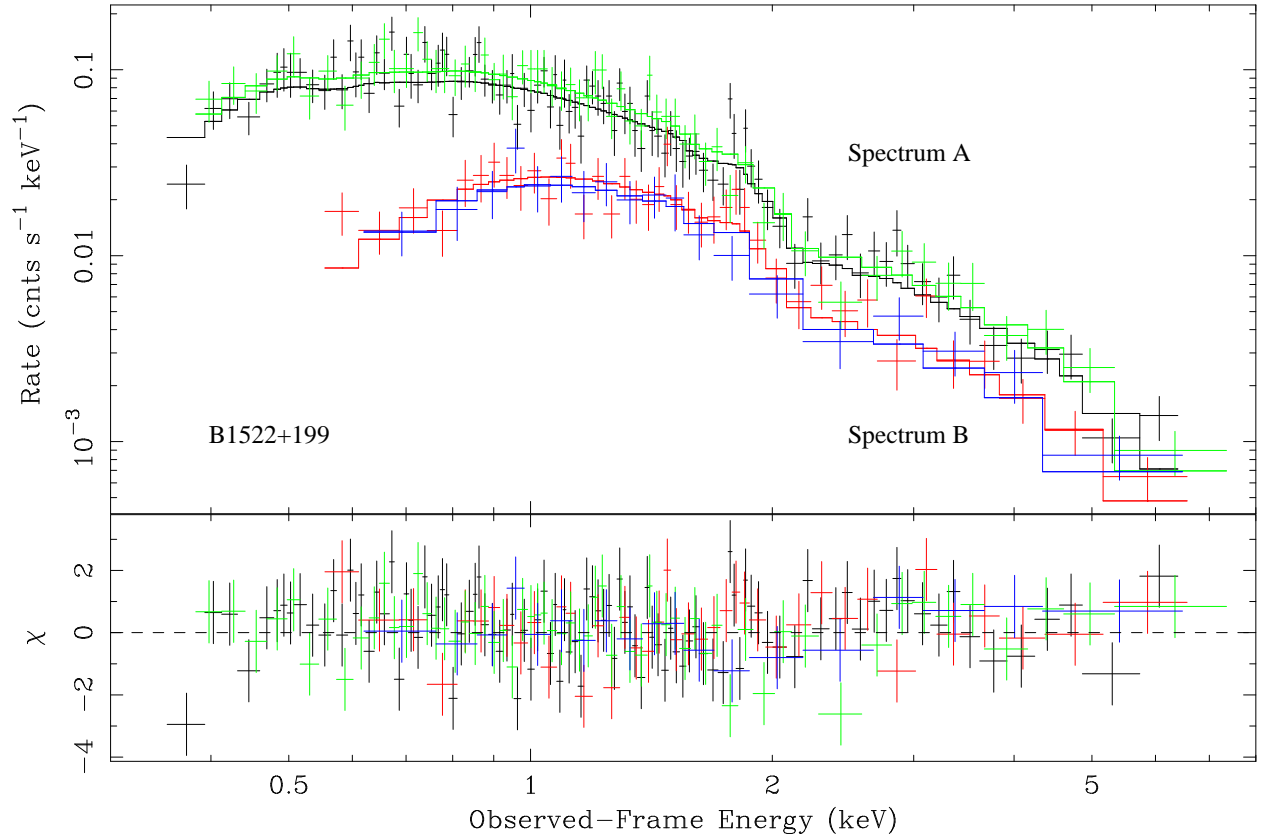


Fig. 4.— Spectra of images A (top) and B (bottom) of B 1152+199 for both *Chandra* observations. The black and red lines are the fits for the spectra A and B in the first *Chandra* epoch, and the green and blue lines are for the second epoch. The lower panel shows the contributions of the residuals to the χ^2 fit statistics.

separately, and obtained consistent differential absorptions for both observations (Table 2). We used the model-averaged extinction of $E(B - V) = 1.20 \pm 0.05$ mag from Elíasdóttir et al. (2006), where the small scatter in the value between their models would have little effect on our results. Combining the differential extinction and absorption measurements, we found a dust-to-gas ratio for the lens galaxy of $E(B - V)/N_{\text{H}} = (2.5 \pm 0.2) \times 10^{-22}$ mag $\text{cm}^2 \text{atoms}^{-1}$. This is the most accurate dust-to-gas ratio measurement we have obtained so far. There is weak evidence (1.4σ) for a change in the X-ray flux ratios, where the flux ratio (A/B) is larger in the second epoch (see Table 2). The X-ray flux ratios after correcting for absorption ($A/B = 1.87 \pm 0.14$ and 2.28 ± 0.25) are also consistent with the range of optical flux ratios after correcting for extinction (e.g., $\Delta M = 0.85 \pm 0.07$, 0.6 ± 0.1 , Elíasdóttir et al. 2006).

4. Discussion

We summarize all available differential absorption measurements in Table 3, including the three results from this paper (SBS 0909+523, FBQS 0951+2635, and B 1152+199) and the five existing measurements from Dai et al. (2006). We find an average dust-to-gas ratio of

$$E(B - V)/N_{\text{H}} = (1.5 \pm 0.5) \times 10^{-22} \text{mag cm}^2 \text{atoms}^{-1} \quad (2)$$

with an intrinsic scatter of $\simeq 40\%$, where we must exclude FBQS 0951+2635 and HE 1104–1805 from the fits. If we allow for no intrinsic scatter, we found a ratio of $(2.3 \pm 0.2) \times 10^{-22}$ mag $\text{cm}^2 \text{atoms}^{-1}$ with $\chi^2/N_{\text{dof}} = 3.0$, indicating the existence of the additional scatter we include in our standard estimate. These estimates are consistent with our previous estimate in Dai et al. (2006) and the average Galactic value of 1.7×10^{-22} mag $\text{cm}^2 \text{atoms}^{-1}$ (Bohlin, Savage & Drake 1978). The estimates for the intrinsic scatter are also consistent with local estimates given our small sample size. We compare the results for the lens galaxies to the local stellar sample from Bohlin, Savage & Drake (1978) in Figure 5, and plot the evolution of dust-to-gas ratios in Figure 6. Contini & Contini (2007) examined this question by modeling the bulk emission of luminous IR galaxies, finding that the dust-to-gas ratio is significantly higher than the Galactic value in star forming and central nucleus regions (see also Maiolino et al. 2001a,b) and consistent with the Galactic value elsewhere. However, the scatter of their results is significantly larger than our more direct measurements. In addition, Menard & Chelouche (2008) found several *MgII* absorbers at $z \sim 1$, which also have dust-to-gas ratios close to the Galactic value. In our present results, we see no evidence for evolution in the dust-to-gas ratio to $z \simeq 1$, and with a larger sample we will be able to test the ISM evolution models of simulations (e.g., Dwek 1998; Edmunds 2001; Inoue 2003).

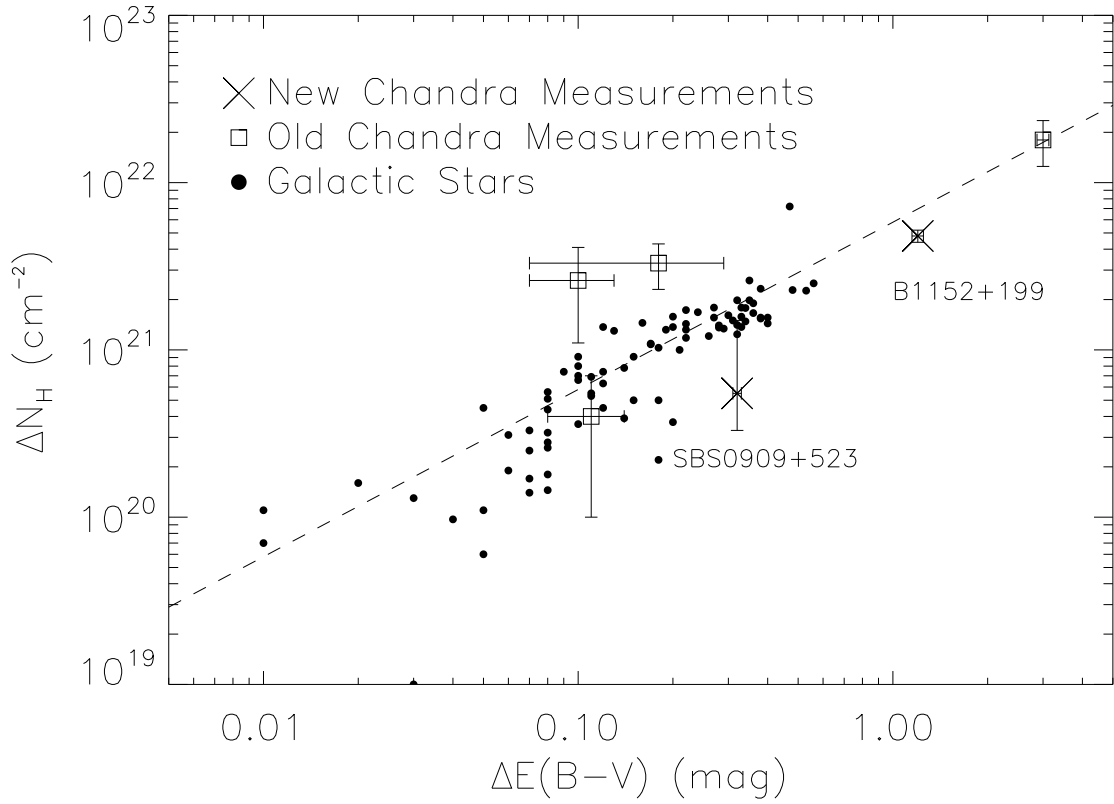


Fig. 5.— ΔN_{H} versus $\Delta E(B - V)$ for the gravitational lenses (squares and crosses) and N_{H} versus $E(B - V)$ for Galactic stars from Bohlin et al. (1978, filled circles). The dashed line shows the mean Galactic relation. The two crosses are the new *Chandra* measurements for SBS 0909+523 and B 1152+199.

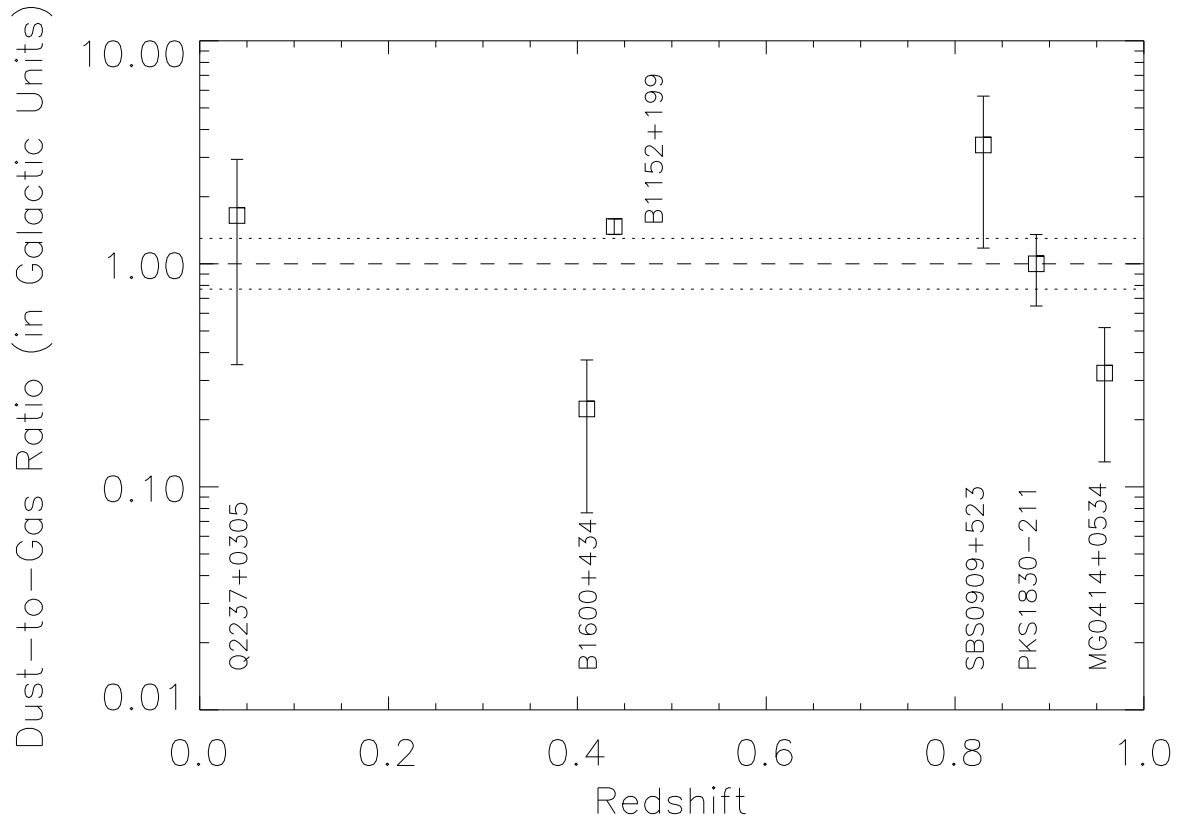


Fig. 6.— The the dust-to-gas ratio (squares) versus redshift in Galactic units of 1.7×10^{-22} mag cm² atoms⁻¹. The dashed and dotted lines show the Galactic value and its intrinsic scatter of 30%.

The primary systematic uncertainty for our results comes from chromatic microlensing of the quasar by the stars in the lens galaxy distorting the optical and X-ray spectra. Given the available information for the systems we consider, it is possible that HE 1104–1805 and FBQS 0951+2635 are affected by this problem while the rest show no evidence of a problem. In addition, since we have confined our studies to systems with significant evidence for extinction, we are relatively safe from minor chromatic microlensing. If microlensing is creating the large color differences between the images then we should also see rapid changes in the colors because a strong chromatic effect requires the source to lie near or on a caustic. Nonetheless, it is possible from two of the systems (HE 1104–1805 and FBQS 0951+2635) that microlensing can mimic extinctions of order $\Delta E(B - V) = 0.1$ mag. However, that the lenses follow the local dust-to-gas ratio and with similar scatter is strong evidence that the remaining systems are little affected by high levels of chromatic microlensing effect. Monitoring these systems at both optical and X-ray wavelengths would allow secure determination of the absorption properties while simultaneously allowing us to determine the spatial structure of the source quasar.

We thank Á. Elíasdóttir, B. Menard, L. J. Goicoechea, and the anonymous referee for helpful comments. We gratefully acknowledge the financial support by CXC grant G07-8080.

Table 3. The Dust-To-Gas Ratio of High Redshift ($z > 0$) Galaxies

Lens	z_l	type	Between Images	ΔN_{H} (10^{22} cm^{-2})	$\Delta E(B - V)$ (mag)	$E(B - V)/N_{\text{H}}$ ($10^{-22} \text{ mag cm}^2 \text{ atoms}^{-1}$)
New Measurements						
SBS 0909+523	0.83	elliptical	B, A	$0.055^{+0.095}_{-0.022}$	0.32 ± 0.01	$5.8^{+3.9}_{-3.7}$
FBQS 0951+2635	0.26	elliptical	B, A	$0.49^{+0.49}_{-0.41}$	-0.12 ± 0.02	... ^a
B 1152+199	0.439	elliptical	B, A	0.48 ± 0.04	1.20 ± 0.05	2.5 ± 0.2
Dai et al. (2006) Sample						
MG 0414+0534	0.9584	elliptical	A, B	0.33 ± 0.10	0.18 ± 0.11	0.55 ± 0.33
HE 1104–1805	0.729	elliptical	A, B	0.055 ± 0.030	-0.07 ± 0.01	... ^a
B 1600+434	0.41	spiral	B, A	$0.26^{+0.17}_{-0.12}$	0.10 ± 0.03	0.38 ± 0.25
PKS 1830–211	0.886	spiral	B, A	$1.8^{+0.5}_{-0.6}$	3.00 ± 0.13	1.7 ± 0.6
Q 2237+0305	0.0395	spiral ^b	A, C	0.04 ± 0.03	0.11 ± 0.03	2.8 ± 2.2

^aThe dust-to-gas ratio was not estimated for FBQS 0951+2635 and HE 1104–1805 because the differential extinction and N_{H} column measurements give opposite signs.

^bQ 2237+0305 is lensed by the central bulge of a spiral galaxy.

REFERENCES

- Anders E. & Ebihara M. 1982, *Geochimica et Cosmochimica Acta* 46, 2363
- Anguita, T., Schmidt, R. W., Turner, E. L., Wambsganss, J., Webster, R. L., Loomis, K. A., Long, D., & McMillan, R. 2008, *A&A*, 480, 327
- Arnaud, K. A. 1996, ASP Conf. Ser. 101: *Astronomical Data Analysis Software and Systems V*, ed. Jacoby G. & Barnes J., 17
- Blackburne, J. A., Pooley, D., & Rappaport, S. 2006, *ApJ*, 640, 569
- Bohlin, R. C., Savage, B. D., & Drake, J. F. 1978, *ApJ*, 224, 132
- Cash, W. 1979, *ApJ*, 228, 939
- Chartas, G. 2000, *ApJ*, 531, 81
- Chartas, G., Agol, E., Eracleous, M., Garmire, G. P., Bautz, M. W., & Morgan, N. D. 2002, *ApJ*, 568, 509
- Chartas, G., Eracleous, M., Dai, X., Agol, E., & Gallagher, S. 2007, *ApJ*, 661, 678
- Chartas, G., Kochanek, C. S., Dai, X., Poindexter, S., & Garmire, G. 2008, arXiv:0805.4492
- Contini, M., & Contini, T. 2007, *Astronomische Nachrichten*, 328, 953
- Corasaniti, P. S. 2006, *MNRAS*, 372, 191
- Dai, X., Chartas, G., Agol, E., Bautz, M. W., & Garmire, G. P. 2003, *ApJ*, 589, 100
- Dai, X. & Kochanek, C. S. 2005, *ApJ*, 625, 633
- Dai, X., Kochanek, C. S., Chartas, G., & Mathur, S. 2006, *ApJ*, 637, 53
- Dai, X., Mathur, S., Chartas, G., Nair, S., & Garmire, G. P. 2008, *AJ*, 135, 333
- Dwek, Eli 1998, *ApJ*, 501, 643
- Dickey, J. M. & Lockman F. J. 1990, *ARA&A* 28, 215
- Draine, B. T. 2003, *ARA&A*, 41, 241
- Edmunds, M. G. 2001, *MNRAS*, 328, 223
- Eigenbrod, A., Courbin, F., & Meylan, G. 2007, *A&A*, 465, 51

- Eigenbrod, A., Courbin, F., Sluse, D., Meylan, G., & Agol, E. 2008, *A&A*, 480, 647
- Elíasdóttir, Á., Hjorth, J., Toft, S., Burud, I., & Paraficz, D. 2006, *ApJS*, 166, 443
- Falco, E. E., Impey, C. D., Kochanek, C. S., Lehár, J., McLeod, B. A., Rix, H.-W., Keeton, C. R., Muñoz, J. A., & Peng, C. Y. 1999, *ApJ*, 523, 617
- Fall, S. M., Charlot, S., & Pei, Y. C. 1996, *ApJ*, 464, L43
- Garmire, G. P., Bautz, M. W., Nousek, J. A., & Ricker, G. R. 2003, *SPIE*, 4851, 28
- Ghirlanda, G., Ghisellini, G., Firmani, C., Nava, L., Tavecchio, F., & Lazzati, D. 2006, *A&A*, 452, 839
- Goicoechea, L. J., Shalyapin, V. N., Koptelova, E., Gil-Merino, R., Zheleznyak, A. P., & Ullán, A. 2008, *New Astronomy*, 13, 182
- Inoue, A. K. 2003, *PASJ*, 55, 901
- Kacprzak, G. G., Churchill, C. W., Steidel, C. C., & Murphy, M. T. 2008, *AJ*, 135, 922
- Kochanek, C. S., Falco, E. E., Schild, R., Dobrzycki, A., Engels, D., & Hagen, H.-J. 1997, *ApJ*, 479, 678
- Kochanek, C. S., Dai, X., Morgan, C., Morgan, N., & Poindexter, S. C. G. 2007, *Statistical Challenges in Modern Astronomy IV*, 371, 43
- Lacey, C. G., Baugh, C. M., Frenk, C. S., Silva, L., Granato, G. L., & Bressan, A. 2008, *MNRAS*, 276
- Lehár, J., et al. 2000, *ApJ*, 536, 584
- Madau, P., Pozzetti, L., & Dickinson, M. 1998, *ApJ*, 498, 106
- Maiolino, R., Marconi, A., Salvati, M., Risaliti, G., Severgnini, P., Oliva, E., La Franca, F., & Vanzi, L. 2001, *A&A*, 365, 28
- Maiolino, R., Marconi, A., & Oliva, E. 2001, *A&A*, 365, 37
- Mediavilla, E., Muñoz, J. A., Kochanek, C. S., Falco, E. E., Arribas, S., & Motta, V. 2005, *ApJ*, 619, 749
- Ménard, B., & Chelouche, D. 2008, *arXiv:0803.0745*

- Morgan, C. W., Kochanek, C. S., Dai, X., Morgan, N. D., & Falco, E. E. 2008, *ApJ*, submitted, arXiv:0802.1210
- Mori, K., Tsunemi, H., Miyata, E., Baluta, C., Burrows, D. N., Garmire, G. P., & Chartas, G. 2001, in *ASP Conf. Ser. 251, New Century of X-Ray Astronomy*, ed. H. Inoue & H. Kunieda (San Francisco: ASP), 576
- Morrison, R. & McCammon, D. 1983, *ApJ*, 270, 119
- Motta, V., Mediavilla, E., Muñoz, J. A., Falco, E., Kochanek, C. S., Arribas, S., García-Lorenzo, B., Oscoz, A., & Serra-Ricart, M. 2002, *ApJ*, 574, 719
- Muñoz, J. A., Falco, E. E., Kochanek, C. S., McLeod, B. A., & Mediavilla, E. 2004, *ApJ*, 605, 614
- Myers, S. T., et al. 1999, *AJ*, 117, 2565
- Nadeau, D., Yee, H. K. C., Forrest, W. J., Garnett, J. D., Ninkov, Z., & Pipher, J. L. 1991, *ApJ*, 376, 430
- Oscoz, A., Serra-Ricart, M., Mediavilla, E., Buitrago, J., & Goicoechea, L. J. 1997, *ApJ*, 491, L7
- Poindexter, S., Morgan, N., & Kochanek, C. S. 2008, *ApJ*, 673, 34
- Pooley, D., Blackburne, J. A., Rappaport, S., & Schechter, P. L. 2007, *ApJ*, 661, 19
- Reeves, J. N. & Turner, M. J. L. 2000, *MNRAS*, 316, 234
- Saez, C., Chartas, G., Brandt, W. N., Lehmer, B. D., Bauer, F. E., Dai, X., & Garmire, G. P. 2008, *AJ*, in press, ArXiv e-prints, 801, arXiv:0801.3599
- Schechter, P. L., Gregg, M. D., Becker, R. H., Helfand, D. J., & White, R. L. 1998, *AJ*, 115, 1371
- Schneider, R., Ferrara, A., & Salvaterra, R. 2004, *MNRAS*, 351, 1379
- Toft, S., Hjorth, J., & Burud, I. 2000, *A&A*, 357, 115
- Tsunemi, H., Mori, K., Miyata, E., Baluta, C., Burrows, D. N., Garmire, G. P., & Chartas, G. 2001, *ApJ*, 554, 496
- Voges, W., et al. 2000, *VizieR Online Data Catalog*, 9029, 0

Weisskopf, M. C., Brinkman, B., Canizares, C., Garmire, G., Murray, S., & Van Speybroeck,
L. P. 2002, PASP, 114, 1

Wucknitz, O., Wisotzki, L., Lopez, S., & Gregg, M. D. 2003, A&A, 405, 445